SOLAR RADIATIVE FLUXES IN THE INHOMOGENEOUS STRATUS CLOUDS

G.A. Titov and E.I. Kas'yanov

Institute of Atmospheric Optics,
Siberian Branch of the Russian Academy of Sciences, Tomsk
Received May 25, 1995

Visible solar radiation transfer in inhomogeneous stratus clouds is considered. We propose a model of stratus clouds which allows us to treat fluctuations of both the extinction coefficient (liquid water content) and the upper cloud boundary height. Influence of stochastic geometry of the upper boundary and the inhomogeneous internal cloud structure on one-dimensional probability density, mean value, variance, and energy spectrum of albedo, transmittance, and their sum is discussed. It is shown that the effects associated with interacting radiative fields within spatial pixels result in violation of an one-to-one correspondence between the optical and radiative characteristics of individual pixel. These effects, resulting in certain specific features in the formation of albedo and transmittance statistics, should be accounted for when developing radiation codes of General Circulation Models and when interpreting the data of field measurements in real clouds.

1. INTRODUCTION

A highly important topic of recent concern has been the study of the relationship between the statistical parameters of optical and radiative characteristics of inhomogeneous stratus clouds. Such an importance is not only because this relationship can be used to derive geophysical information (cloud spatial structure, incloud turbulence, etc.), but also because there is a need for improvements of the radiation codes of the general circulation models (GCMs).

A cascade model has been created in the Goddard Space Flight Center (GSFC) to treat stratocumulus clouds with a simplest geometry (plane-parallel layer) and horizontal fluctuations of the liquid water path (optical thickness). These fluctuations have been modeled using a one-dimensional lognormal distribution and a power-law spectrum.[1] It was shown that the area-average albedo essentially depends on the spatial distribution of the optical thickness.[2]

In fact, stratus clouds have a very odd and irregular upper boundaries. Thus, a question arises how strong is influence of stochastic geometry of clouds on one-dimensional probability density, mean value, variance, and energy spectrum of cloud albedo and transmittance for visible solar radiation. In this paper we are trying to address this question using the GSFC model extended to allow for the random behavior of the upper boundary of a cloud layer.

2. CLOUD MODEL

At present no data on simultaneous measurements of the distributions of cloud liquid water and height of the cloud upper boundary can be found in the literature, so the relationship between microphysical and geometrical cloud characteristics has not been experimentally justified. For this reason, we have assumed that the cloud liquid water path and the height of the cloud upper boundary are independent random fields.

The statistical characteristics describing fluctuations of the upper boundary are obtained from laser sensing of stratus clouds over Barents and Norwegian seas in October-November 1987 (Ref. 3). Examples of 1-D probability density and correlation function for a single observation of cloud field cross-section are presented in Fig. 1. This demonstrates that, to a rough approximation, the section of the stratus cloud upper boundary can be modeled by Gaussian process with the exponential correlation function. The correlation radius as determined at e^{-1} level is 2.5–3.5 km. With the limited experimental data, the approximation cannot be improved, and the stratus cloud upper boundary isotropy and homogeneity cannot be justified. So we will model the stratus upper boundary approximately, by homogeneous isotropic Gaussian field with the exponential correlation function.

Below we use the following abbreviation for simplicity:

LWP model describes fluctuations of the liquid water path (optical thickness) in a plane-parallel cloud

0235-6880/95/12 1028-07 $02.00

layer. The LWP fluctuations obey a one-dimensional lognormal distribution and have power-law spectrum;

CUB model describes the fluctuations of the cloud layer upper boundary. The CUB fluctuations are assumed to be a Gaussian process with the exponential correlation function;

LC model is a superposition of the LWP and CUB models and describes fluctuations of both the liquid water content (extinction coefficient) and the cloud upper boundary.

Designations used for statistical characteristics of the optical depth (τ), albedo (R), transmittance (Q), etc., include subscripts (for a model), overbar (for the area average), and symbol Var (for the variance); e.g., R_{LWP} and $\mathrm{Var}\, R_{\mathrm{LWP}}$ denote the area-average and the variance of albedo in LWP model.

For simplicity and for saving computer time, we consider one-dimensional models, that is those in which the optical depth, albedo and transmittance are random processes. Algorithm of simulating LWP, CUB, and LC realizations is based on the method of "spectrum randomization"[4,5] which involves the following steps.

1) LWP model. Plane-parallel layer with the thickness $\Delta H = 0.3$ km and length $L = \mathrm{d}x \cdot N = 204.8$ km is divided into $N = 2^{12}$ pixels (cells) of the same horizontal size $\mathrm{d}x = 0.05$ km. For each pixel, we simulate the optical thickness τ_{LWP} using a one-dimensional lognormal distribution ($\tau_{\mathrm{LWP}} = 13$, $\mathrm{Var}\, \tau_{\mathrm{LWP}} = 25.1$) and a power-law spectrum (with the exponent $\beta = 5/3$). Each pixel is then assigned the extinction coefficient $\sigma(i) = \tau_{\mathrm{LWP}}(i)/\Delta H$, $i = 1, N$.

2) CUB model. Height of the upper boundary, $H(i)$, $i = 1, N$, is simulated with a one-dimensional Gaussian distribution ($H = 0.3$ km, $\mathrm{Var}\, H = 0.01$ km^2) and exponential correlation function (correlation radius 2.5 km). The optical thickness of each pixel is given by $\tau_{\mathrm{CUB}}(i) = H(i) \cdot \overline{\tau}_{\mathrm{LWP}}/\Delta H$, $i = 1, N$.

3) LC model. Each pixel has the extinction coefficient $\sigma(i)$, thickness $H(i)$, and optical thickness $\overline{\tau}_{\mathrm{LC}}(i) = \tau(i) \cdot H(i)$, $i = 1, N$. Owing to the independence of the random processes considered, $\overline{\tau}_{\mathrm{LC}} = \overline{\tau}_{\mathrm{LWP}} = 13$.

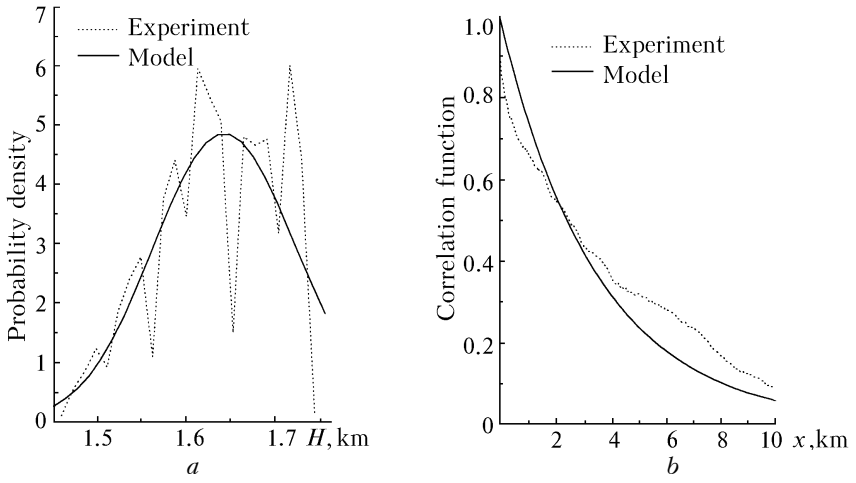

FIG. 1. One-dimensional probability density (a) and correlation function (b) of the height of the cloud upper boundary. Measurements (dashed lines) and approximation (solid lines) by Gaussian distribution function (a) and exponential correlation function $K = \exp(-x/3.5)$ *(b).*

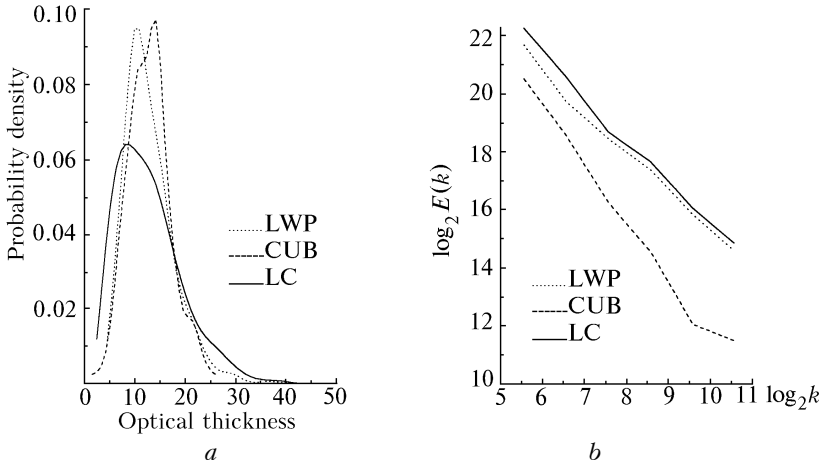

FIG. 2. Probability density (a) and energy spectrum (b) of the optical depth for different cloud models.

Examples of the one-dimensional distributions and energy spectra of optical depth are presented in Fig. 2. Noteworthy, the distribution mode in LC model is shifted toward smaller optical thicknesses and is about 30% smaller, while the distribution itself is broader (Var $\tau_{LC} \approx 2$ Var τ_{LWP}) (see Fig. 2*a* and Table I). Figure 2*b* is a log plot of the energy spectrum of optical thickness, $E(\tau, k)$, as a function of the bin number, k, which is related to the spatial frequency f_k as $f_k = k/L = k/(dx \cdot N)$, where L is the length of the realization processed. In the spatial frequency range under consideration, the energy spectrum $E(\tau_{CUB}, k)$ has nearly smooth (on a log plot) section, which can be approximated by $E(\tau_{CUB}, k) \sim k^{-\beta_{CUB}}$, with $\beta_{CUB} = 1.9$; that is, $\beta_{CUB} > \beta_{LWP}$ and $E(\tau_{CUB}, k)$ falls off faster than $E(\tau_{LWP}, k)$. Since the variance of τ_{LWP} is 1.5 times larger than that of τ_{CUB}, the energy spectrum $E(\tau_{LC}, k)$ only slightly differs from $E(\tau_{LWP}, k)$.

TABLE I. Variances, minimum (Min), maximum (Max), and mean values of the optical depth (τ), albedo (R), transmittance (Q), and their sum ($R+Q$), corresponding to the LC and LWP cloud models. Values in parentheses refer to the radiative characteristics obtained with Var $\tau_{LWP} = 47.3$.

Parameter	Model	Min	Max	Mean	Variance
τ	LC	0.45	60.30	13.08	47.30
	LWP	3.06	44.90	13.03	25.10
R	LC	0.179	0.784	0.478	0.012
	LWP	0.241	0.762	0.492	0.007
		(0.175)	(0.828)	(0.477)	(0.012)
Q	LC	0.177	1.039	0.522	0.022
	LWP	0.219	0.966	0.508	0.011
		(0.161)	(1.112)	(0.523)	(0.019)
$R + Q$	LC	0.796	1.338	1.0	0.005
	LWP	0.887	1.224	1.0	0.001

3. ALBEDO AND TRANSMITTANCE

Albedo and transmittance are computed for each pixel by Monte Carlo method, employing, in particular, the Maximum Cross Section Method.[6] The calculations have been made for the overhead sun and Heneye-Greenstein scattering phase function with the asymmetry parameter of 0.843. Impacts of the underlying surface and aerosol atmosphere have not been accounted for. In order to evaluate the extreme possible impact of the cloud top stochasticity on the solar radiation transfer in the inhomogeneous stratus clouds, R_{LC} and Q_{LC} were calculated with Var H = = $(\bar{H}/3)^2 = 0.01$ km^2. Minimum and maximum (H_{max}) cloud top heights were, respectively, 0.014 and 0.646 km. The transmittances Q_{LWP} and Q_{LC} are calculated at the level of the cloud lower boundary (plane $z = 0$). Most of R_{LWP} computations refer to the altitude $z = \Delta H$, while R_{LC} is computed at the maximum level of the cloud upper boundary (plane $z = H_{max}$); untill otherwise is noted in figure captions (see e.g., Figs. 7*a*,*b*). The relative computation error was within 1%.

Below we present the calculational results which illustrate the influence of stochastic geometry of stratus cloud upper boundary, upon the statistical characteristics of albedo and transmittance. Note that these effects, completely missing in LWP model, are most important for cumulus clouds and are thoroughly discussed in Refs. 7–9.

Examples of the realizations of optical depth, albedo, transmittance, and their sum $R + Q$ are given in Fig. 3, from which we see that maximum (minimum) pixel optical depth is larger (lower) in LC than in LWP model. This might explain the increase (decrease) of the maximum (minimum) values of albedo, transmittance, and their sum in the stratus clouds with random upper boundary.

For pixels nearly as tall as wide or taller, the radiation interaction associated with the horizontal photon transport substantially affects albedo and transmittance. These latter depend on optical properties of an ensemble of pixels, rather than on parameters of a single pixel. For example, pixels of the same optical thicknesses (Fig. 3*a*, points *A* and *B*) possess different albedo values (Fig. 3*b*, points *C* and *D*).

Multiple scattering tends to smooth the radiation fields, so that albedo has a more uniform spatial distribution than the optical depth (Fig. 3*a*, *b*). In LC model the albedo of each pixel is calculated in the plane $z = H_{max}$. Radiative field reflected by a pixel with $H < H_{max}$ spreads in the space before reaching the plane $z = H_{max}$ to give albedo. In addition, it overlaps with neighboring pixels' radiative fields. Both these effects further smooth the reflected solar radiation fields, so that $R_{LC}(x)$ does not reproduce essential details in $\tau_{LC}(x)$ pattern. In contrast, transmittance is calculated at the cloud base being the same for all pixels; thus the spread and overlap effects do not work now. This circumstance, as well as the strong forward peak of the scattering phase function and the contribution from direct solar radiation, leads to transmittance being more sensitive to spatial variability of the optical depth than albedo (Figs. 3*a*,*b*,*c*).

Cloud top is illuminated by a parallel unit solar flux (homogeneous boundary conditions), thus for each pixel in horizontally homogeneous clouds the balance of radiant energy holds, which for the conservative scattering case assumes that $R + Q = 1$. Unlike, in the horizontally inhomogeneous clouds, the radiant energy balance holds on the average, while $R + Q$ in an individual pixel may substantially differ from unity (Fig. 3*d*). We see that certain relationships from classic radiative transfer theory may break down in inhomogeneous cloud systems that should be kept in mind when interpreting data on real clouds. In our opinion, the theory of radiative transfer in horizontally inhomogeneous clouds and, in

particular, the effect of local deviation of radiant energy balance from unity is of a key importance for understanding of the cloud absorption anomaly what is intensively debated among the scientific community now.[10,11]

The account for random upper boundary changes a little bit the mean albedo and transmittance, while almost doubling their variances (Table I) and appreciably affecting the probability densities (Fig. 4). Obviously, the cause of the differences is in the fact that $\mathrm{Var}\,\tau_{LWP} < \mathrm{Var}\,\tau_{LC}$. Computational results for albedo and transmittance in the LWP model with $\mathrm{Var}\,\tau_{LWP} = \mathrm{Var}\,\tau_{LC}$ are given in Table I (in parentheses) and show that, at fixed mean value and variance of optical depth, the mean and the variance of albedo and transmittance depend only a little on the cloud model. The probability density of R_{LC}, unlike that of R_{LWP}, is distinctly bimodal (Fig. 4*a*).

The shape of the probability density of $R + Q$ essentially differs from δ-function, which represents the probability density in the case of horizontally homogeneous clouds (Fig. 5*a*). In order to quantify the contributions from optically thin and thick pixels to the $R + Q$ values higher (lower) than unity, all the $R + Q$ sums calculated in LC model were divided into two arrays, one with $(R + Q)$s from thinner than mean pixels ($\tau < 13$), and another from those with $\tau > 13$. The resulting arrays were then statistically processed to evaluate the contribution from each of them to the probability density. The results are presented in Fig. 5*b*. The radiation incident upon the optically denser ($\tau > 13$) pixels slides down to the optically thinner ones. The former, relatively stronger reflecting pixels often possess lower radiant energy ($R + Q < 1$), while the latter ($\tau \le 13$), normally gaining radiation from the adjacent, optically denser pixels and capable of transmitting much of the solar flux, possess excessive radiant energy ($R + Q > 1$).

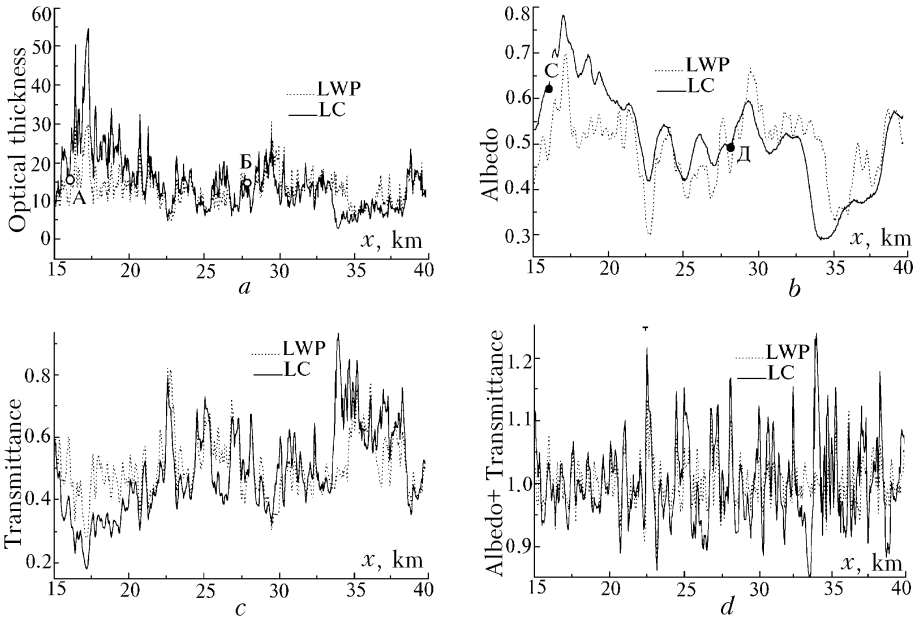

FIG. 3. Examples of realizations of optical depth (a), albedo (b), transmittance (c), and albedo plus transmittance (d). LC model (solid lines) and LWP model (dashed lines).

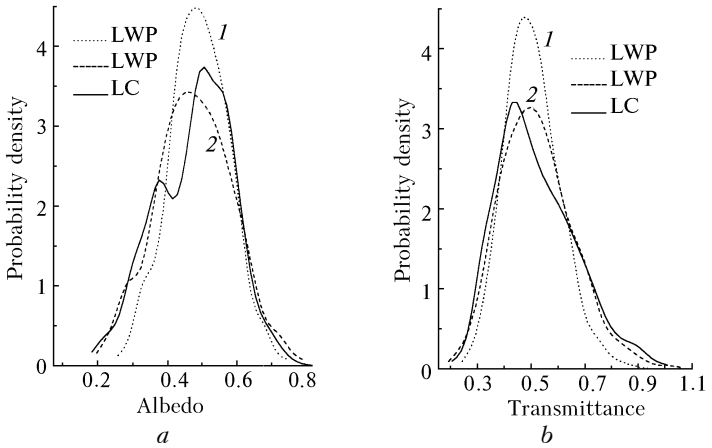

FIG. 4. Probability densities of albedo (a) and transmittance (b): $\mathrm{Var}\,\tau_{LWP} = 25.1$ *(1) and* $\mathrm{Var}\,\tau_{LWP} = \mathrm{Var}\,\tau_{LC} = 47.3$ *(2).*

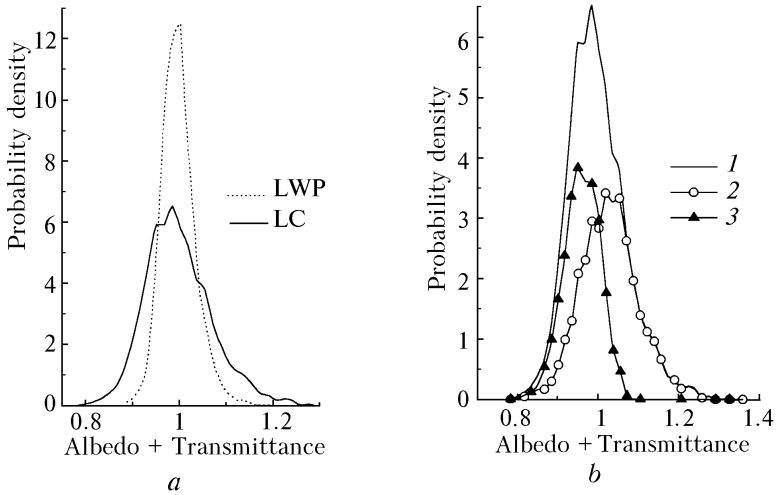

FIG. 5. Probability density of albedo plus transmittance (a) and the components of the probability density of $R_{LC} + Q_{LC}$ (b): (a) $R_{LC} + Q_{LC}$ (solid), $R_{LWP} + Q_{LWP}$ (dashed); (b): probability density of $R_{LC} + Q_{LC}$ (1) and its components due to pixels with optical thicknesses τ□< 13 (2) and τ□> 13 (3).

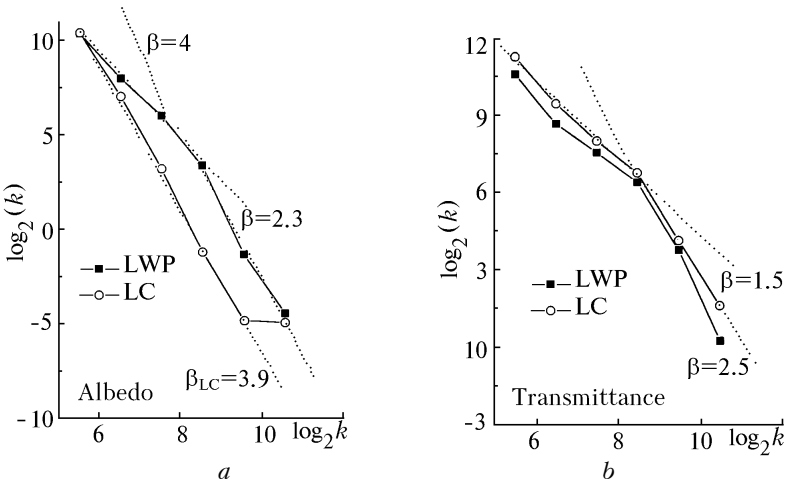

FIG. 6. Energy spectra of albedo (a) and transmittance (b) for LC and LWP models.

Energy spectrum of the optical depth varies a little between those for LWP and LC models (Fig. 2*b*), whereas the energy spectra of R_{LWP} and R_{LC} substantially differ (Fig. 6*a*). The overlap and spread effects smoothen the radiation fields reflected by individual pixels so that the slope of the energy spectrum of R_{LC} is larger (larger correlation length) than that of R_{LWP}. There can occur the scaling break in the energy spectra of reflected intensity[12] and albedo[13] at spatial scales on the order of several hundred meters. Our results confirm this fact and show that the energy spectrum of transmittance is broken as well (Fig. 6*b*). The explanation is that the multiple scattering effectively smoothens the radiative field at spatial scales on the order of ten photon mean-free paths. For the given model parameters, an appreciable contribution to Q_{LC} may come from direct radiation, whose spatial distribution follows that of τ_{LC}. Owing to the strong forward peak of the scattering phase function, the transmitted radiation field is smoothened by multiple scattering to a lower degree than the reflected field. All pixels have the same base height at which the transmittance is calculated. For these reasons the spatial spectra $E(R_{LC}, k)$ and $E(Q_{LC}, k)$ substantially differ from each other.

It very hard in practice to perform airborne albedo measurements exactly at a maximum height of the cloud upper boundary, H_{max}. So, let an aircraft fly at a height H_R above the plane $z = H_{max}$. As H_R increases, the spread and overlap effects of the reflected radiation fields increasingly smoothen the spatial distribution of albedo, so that its small scale fluctuations vanish (Fig. 7*a*,*b*) and its probability density contracts in shape (Fig. 7*c*,*d*).

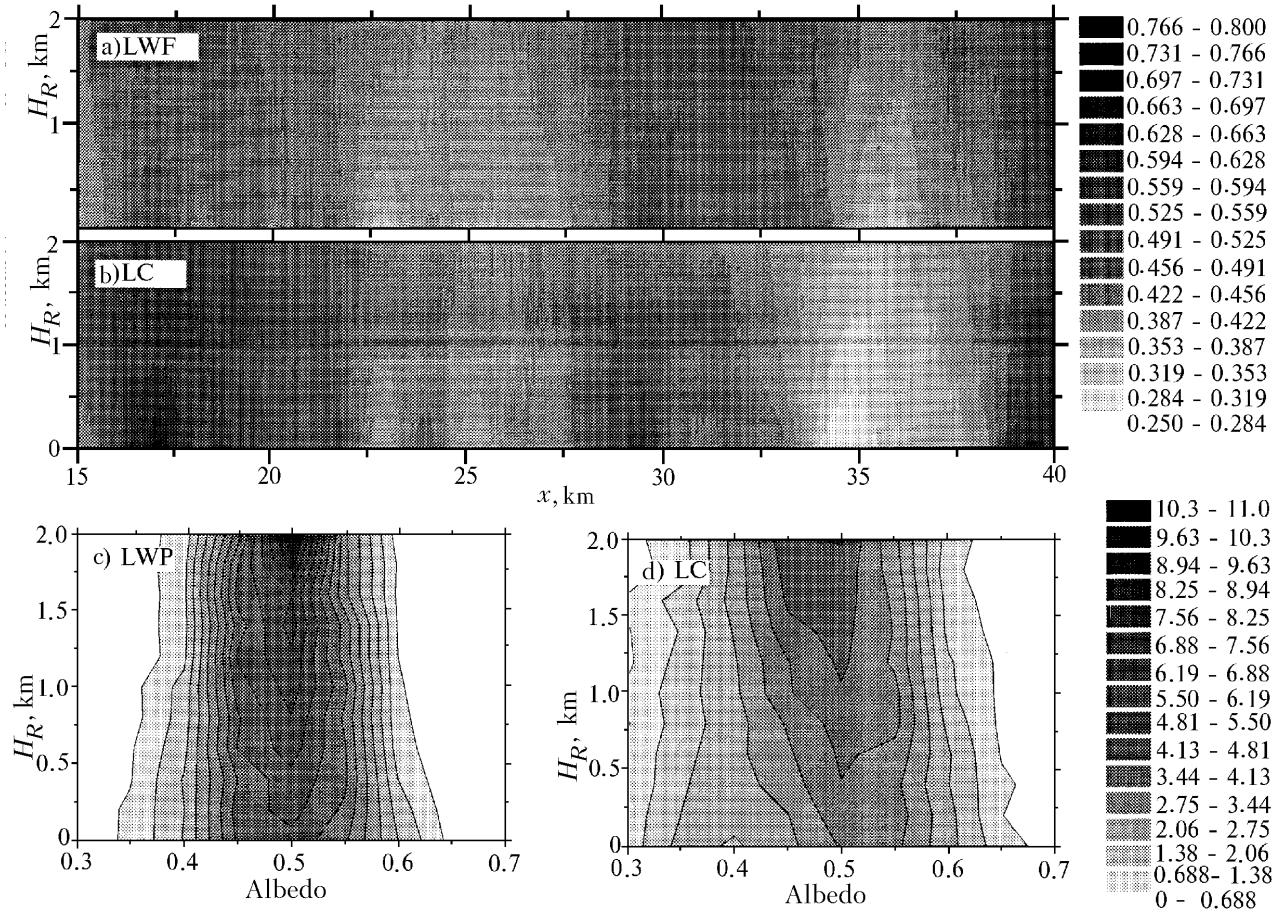

FIG. 7. Examples of albedos R_{LWP} (a) and R_{LC} (b) for different heights H_R (plane $z = H_R$) and the dependence of the probability density of albedo R_{LWP} (c) and R_{LC} (d) on the height H_R. The height H_R is measured from the level $z = H_{max}$ *($z = H_R = 0$ corresponds to $z = H_{max}$).*

4. CONCLUSION

The calculational results show that, at fixed mean value and variance of the optical depth, the mean value and variance of the albedo and transmittance depend weakly, while the probability density and energy spectrum of albedo depend strongly, on the effects associated with the stochastic geometry of the upper boundary of inhomogeneous stratus clouds.

The radiative field is effectively smoothened by multiple scattering at the spatial scales on the order of ten photon mean-free paths, so that scaling break in energy spectra of albedo and transmittance can occur at spatial frequencies corresponding to the inhomogeneities on the order of several hundred meters in size.

Because of the spread and overlap of radiation fields of individual pixels, the albedo (transmittance) statistics essentially depends on the distance between the receiver and the upper (lower) cloud boundary.

There is a strong horizontal variability of albedo and transmittance in inhomogeneous stratus clouds, so that the radiant energy balance holds on the average, for the entire realization, but may break down for each individual pixel. Addition of stochastic upper boundary amplifies the horizontal variability of the albedo and transmittance.

ACKNOWLEDGMENTS

The authors would like to thank A. Marshak, A. Davis, W. Wiscombe (NASA GSFC), and S. Prigarin (SB RAS Computer Center) for fruitful discussions of the results presented in this paper.

The research was supported by the DOE's ARM Program under Contract No. 350114-A-Q1, Russian Foundation for Fundamental Research Grant No. 95-05-14162, and International Scientific Foundation Grant No. JJ7100.

REFERENCES

1. R.F. Cahalan, in: *Advances in Remote Sensing Retrieval Method* (Deepark Pub., 1989), pp. 371–388.
2. R.F. Cahalan, W. Ridgway, W.J. Wiscombe, T.L. Bell, and J.B. Snider, J. Atmos. Sci. **51**, 2434–2455 (1994).
3. I.G. Andrianov, I.E. Penner, G.A. Titov, and V.S. Shamanaev, in: *Abstracts of Reports at the First*

Interrepublic Symposium on Atmospheric and Oceanic Optics (Tomsk, 1994), pp. 238–240.
4. G.A. Mikhailov, Dokl. Akad. Nauk SSSR **238**, No. 4, 793–795 (1978).
5. G.A. Mikhailov, Zh. Vychisl. Mat. Mat. Fiz. **23**, No. 3, 558–566 (1983).
6. G.I. Marchuk, G.A. Mikhailov, N.A. Nazaraliev, et al., *Monte Carlo Method in Atmospheric Optics* (Nauka, Novosibirsk, 1976), 283 pp.
7. G.A. Titov, J. Atm. Sci. **47**, No. 1, 24–38 (1990).
8. V.E. Zuev and G.A. Titov, J. Atm. Sci. **51**, No. 12, 176–190 (1995).
9. V.E. Zuev and G.A. Titov, Atmos. Oceanic Opt. **8**, Nos. 1–2, 105–115 (1995).
10. R.D. Cess, M.H. Zhang, P. Minnis, et al., Science **267**, 496–499 (1995).
11. V. Ramanathan, B. Subasilar, M.H. Zhang, et al., Science **267**, 499–503 (1995).
12. H.W. Barker and J.A. Davies, Remote Sens. Environ. **42**, 51–54 (1992).
13. R.F. Cahalan and J.B. Snider, Remote Sens. Environ. **28**, 95-107 (1989).